Int J Adv Manuf Technol (2015) 81:1509–1518
DOI 10.1007/s00170-015-7319-4

ORIGINAL ARTICLE

Modelling of the ball burnishing process with a high-stiffness tool

Sasa Randjelovic[1] · Branko Tadic[1] · Petar M. Todorovic[1] · Djordje Vukelic[2] · Danijela Miloradovic[3] · Milan Radenkovic[1] · Christos Tsiafis[1]

Received: 11 December 2014 / Accepted: 13 May 2015 / Published online: 26 May 2015

Abstract This paper deals with the problem of forming a surface roughness profile of a machined surface and a definition of the optimal depth of penetration in ball burnishing which would allow minimization of surface roughness. The assumptions, which have been numerically and experimentally verified, claim that maximum surface quality, i.e., minimum surface roughness, Ra, is achieved when the depth of ball penetration into the workpiece material is approximately equal to the maximum peak height, Rp. For the purpose of numerical simulations, a surface roughness model based on milling kinematics was used. Numerical simulations and the used roughness model support the claim that penetrating with a stiff tool up to the mean line of the roughness profile yields best surface quality. The authors maintain that ball penetrations, which exceed Rp, cannot significantly improve surface quality. Furthermore, the phenomenon of profile peak deformation is substantially clarified. The analysis of internal stresses within the workpiece after ball burnishing allowed a relationship to be established between internal stress distribution along the depth of the hardened layer and ball penetration depth.

Keywords Ball burnishing · FEM analysis · Surface roughness · Residual stresses

✉ Petar M. Todorovic
petar@kg.ac.rs

[1] Department for Production Engineering, Faculty of Engineering, University of Kragujevac, Kragujevac 34000, Serbia

[2] Department for Production Engineering, Faculty of Technical Sciences, University of Novi Sad, Novi Sad 21000, Serbia

[3] Department for Motor Vehicles and Motors, Faculty of Engineering, University of Kragujevac, Kragujevac 34000, Serbia

1 Introduction

Ball burnishing is a cold finishing process in which a ball is rolled over the workpiece surface. Contact pressures cause plastic deformation of the workpiece surface layer. A plastic flow of surface roughness profile peaks takes place, thus filling the adjacent valleys. In this process, the rough surface texture is evened out and becomes smoother. The described method also contributes to formation of hard surface layers due to deformation strengthening. Under certain conditions, ball burnishing is a good alternative for processing and can be applied for the treatment of workpieces of different materials. Using ball burnishing as a final processing, operation allows certain workpiece surfaces to have improved wear resistance, corrosion resistance, fatigue, tensile strength, etc.

Many investigations of burnishing processes have been focused on the ball burnishing process, due to its advantages, such as flexibility, simplicity, cost-effectiveness, etc. Previous investigations have been mostly focused on the development of analytical and empirical regression models, as well as the application of optimization methods (response surface methodology, Taguchi method) and the application of artificial intelligence, the finite element method (FEM) and practical experiments.

Literature reviews show that many studies focus on the development of analytical models. Bouzid et al. [1] defined an analytical model to determine the roughness of burnished surfaces in relation to the feed rate, the depth of penetration and the roughness of the initial surface obtained by turning or grinding. The normal displacement has been calculated using the Hertz contact theory which supposes that the behaviour of the workpiece material is elastic. Bougharriou et al. [2] performed analytical modelling and FEM analysis to study burnishing on an AISI 1042 workpiece. The simulations were made to analyze the surface profile, the residual stresses and

the influence of burnishing parameters on surface roughness and the residual stress distribution. Li et al. [3] proposed an analytical model for surface roughness during the burnishing process. They proposed a burnishing mechanism in which the geometries of the burnishing tool and workpiece, the microscopic topography of the surface and the mechanical properties of the workpiece were taken into consideration. The model allowed insight into the influence of the burnishing force on burnishing surface roughness and the closed form solution of the lowest surface roughness and optimum burnishing force. Gharbi et al. [4] developed an analytical model to predict surface roughness as the function of speed, force and feed rate. The results showed that the burnishing of aluminium 1050A plates improved its ductility, but not its microhardness. Bougharriou et al. [5] performed an analytical model to predict the surface profile obtained by ball burnishing after turning. The quality of the generated surface was supposed to depend on several parameters like the cutting parameters, the tool geometry, the workpiece material, the tool wear resistance and the relative vibration between the tool and the workpiece during turning and burnishing.

Empirical models (regression models) based on collected experimental data have also been implemented by several researchers. Rao et al. [6] established the effects of ball burnishing parameters on the surface hardness of high-strength low-alloy steel dual-phase steel specimens. Statistical analysis showed that the speed, feed, lubricant and ball diameter had a significant effect on surface hardness. Abu Shreehah [7] evaluated the effect of different burnishing conditions on surface microhardness, surface roughness and form accuracy. Optimum burnishing parameters were established which minimized roughness and/or maximized surface hardening. Empirical formulas were developed to predict the surface microhardness and roughness of leaded brass obtained by burnishing. Sagbas [8] presented a strategy based on the desirability function approach together with response surface methodology to optimize the ball burnishing process. The burnishing force, number of passes, feed rate and speed were considered as model variables. The results indicated that burnishing force and number of passes were the significant factors for surface roughness. Tadic et al. [9] discussed the effects of the ball burnishing process taking into consideration the initial surface roughness. Burnishing was performed using an especially designed high-stiffness tool. The authors assumed that, compared to its previous counterparts with coiled springs, a high-stiffness tool should increase surface quality.

In order to properly optimize the burnishing process, several investigations have been based on response surface methodology and the Taguchi method. El-Taweel and El-Axir [10] experimentally studied the effect of some parameters in the ball burnishing process on surface microhardness and roughness. The Taguchi method was employed to explore the influences of burnishing parameters (speed, feed, force and number of passes) on the improvement ratio of surface roughness and the ratio of surface microhardness. Esme [11] investigated multi-response optimization of the burnishing process for an optimal parametric combination, yielding favourable surface roughness and microhardness, using the Grey relational analysis and Taguchi method. The significance of burnishing parameters in regard to the quality characteristics of the burnishing process was evaluated with an analysis of variance. Babu et al. [12] evaluated the effects of various burnishing parameters on the surface characteristics, surface microstructure and microhardness. The Taguchi technique was employed in this investigation to identify the most influential parameters on surface roughness. Revankar et al. [13] used the Taguchi method for the optimization and analysis of burnishing parameters (burnishing speed, feed, force and number of passes) on the output responses' surface roughness and surface hardness. The optimization results revealed that burnishing feed and speed are significant parameters for minimizing the surface roughness, whereas burnishing force and number of passes play important roles in maximizing the hardness.

Due to its tolerance to imprecision, uncertainty and approximation techniques, artificial intelligence has also been implemented by several researchers to investigate the ball burnishing approach. Esme et al. [14] developed a surface roughness prediction model using an artificial neural network (ANN) to investigate the effects of burnishing conditions during machining of AA 7075. The ANN model of surface roughness parameters was developed with consideration to the burnishing force, number of passes, feed rate and speed. Ibrahim et al. [15] examined the use of a ball burnishing tool (follower rest) to achieve good surface characteristics, such as a higher surface finish and lower out-of-roundness. The effects of three burnishing parameters (burnishing speed, feed and force) on the out-of-roundness were studied. Experimental results were used as a knowledge base to prepare a fuzzy logic model which controls burnishing parameters. Basak and Goktas [16] discussed the effect in which the number of revolutions, feed, number of passes and pressure force exert on surface roughness and surface hardness in Al 7075-T6 materials. A Fuzzy logic model was used to predict the best parameters for the burnishing process. Esme et al. [17] used regression and neural network techniques to predict surface roughness in the ball burnishing process. Effects of the main burnishing parameters on surface roughness were determined. Stalin John and Vinayagam [18] used the Sugeno fuzzy neuro system to model the nonlinear characteristics of the surface roughness (along the tool path and across the tool path) and microhardness. For aluminium alloy, their experiment showed that surface roughness is less along the tool path than across the tool path after the ball burnishing process. Sarhan and El-Tayeb [19] developed a fuzzy rule-based system for prediction of burnished surface roughness. A fuzzy logic-based model was used to predict the surface roughness for a burnished brass surface.

The experimental results showed that increasing burnishing speed and depth has a negative impact on the improvement of surface roughness, Ra, especially at higher feed rates.

Due to high nonlinearity of the ball burnishing problem, numerical models, i.e. FEM simulations, have found significant application in the analysis of burnishing processes. Bouzid Sai and Sai [20] analyzed surface roughness of an AISI 1042 steel workpiece under the ball burnishing process. They created a finite element (FE) model in which the elasto-plastic behaviour of the workpiece was taken into account to determine material displacement. The model permitted the calculation of the residual stresses related to the contact geometry. Balland et al. [21] proposed two FE models of ball burnishing for surface topology based on a smooth cylinder and an irregular surface. The effect of the burnishing process on the material was analyzed. It was observed that the mechanism of formation and flow of the ridge played a key role, but the numerical models were inaccurate in predicting surface geometries and mechanical characteristics. Sayahi et al. [22] presented 2-D and 3-D FE modelling of the ball burnishing process. An elasto-plastic material model was assumed in the framework of the FE analysis. The pertinence of these models to predict residual stresses created by the process was discussed by drawing comparisons between simulation results and experimental data. Grochała et al. [23] presented the effects of modelling the stress in the burnished surface that had been previously milled. A spatial kinematic-geometric model of the surface structure after milling was used. Mohammadi et al. [24] developed an FE model to simulate a low plasticity burnishing process. The model was used to investigate the effect of the main parameters (ball diameter, burnishing force, burnishing feed and number of passes) on the resultant profile of residual stress and plastic deformation. The design of the experiment and response surface methodology was used to develop response functions to approximate the residual stress profile and plastic deformation.

Experimental studies were the subject of study of most researchers. Experimental studies were included to investigate the impact of the most important parameters of ball burnishing, as well as the analysis of the obtained results. El-Axir [25] studied the relationships between the fatigue life, residual stress and ball burnishing process parameters. Experimental work was focused on establishing the effect of burnishing parameters (burnishing speed, force and feed) on the residual stress and fatigue life of aluminium alloy 6061-T6. The residual stress distribution in the surface region due to ball burnishing was determined using a deflection-etching technique. El-Tayeb et al. [26] designed tools with an interchangeable adapter for burnishing. Ball burnishing processes were performed on aluminium workpieces with different parameters and different burnishing orientations to investigate the role of burnishing speed, burnishing force and burnishing tool dimension on the surface qualities and tribological properties. Grzesik and Zak [27] presented a sequential process which incorporates optionally CBN turning operations with or without cryogenic pre-cooling of the workpiece and ball burnishing operations. SEM/BSE and EDS techniques were employed to document the synergic effects of cryogenic treatment prior to turning and ball burnishing operations. The integrity, microhardness and microstructure of the surface were examined.

Most of the previously discussed investigations were focused on the effects of ball burnishing parameters on surface integrity, such as residual stresses, surface hardness and surface roughness. These investigations have mostly been focused on the effects of process parameters (pressure, force, speed, feed rate, number of passes, ball diameter, lubricant, etc.) on the surface integrity. Each of these investigations has had its advantages and disadvantages. Analysis of previous investigations reveals that methodologies developed so far lack universality. More precisely, it is difficult to draw general conclusions about the various ball burnishing phenomena. For example, experimental investigations yield reliable information on the process. However, the results of one experiment cannot be directly compared to another experiment which uses different machining/treatment conditions. The problem of universality also appears in the domain of analytical, empirical and FEM models. FEM models are useful because of their ability to cover a wide range of variables, i.e. including most of the ball burnishing parameters. On the other hand, each FEM model is specific to a particular case of ball burnishing treatment. Analytical and empirical models are also incapable of taking all the required parameters into consideration. In general, each particular method of investigation is limited in one way or another. In the research [28], the problem of optimal depth of ball penetration into the workpiece material from the aspect of minimum arithmetic mean surface roughness, Ra, has been introduced. This parameter was determined experimentally for the specific conditions of ball burnishing. However, the research lacked universal application. The research results were not verified for a wider range of possible treatment conditions (workpiece material, type of previous machining, etc.).

In contrast to previous investigations, the focus in this paper is placed on the development of a more universal methodology. The main goal of this investigation is based on a premise that the initial surface roughness prior to application of the ball burnishing treatment has no significant effect on the surface quality achieved by ball burnishing. Moreover, the minimal surface roughness after ball burnishing can be achieved by penetrating the workpiece surface up to the depth equivalent to maximum peak height, Rp, regardless of the particular burnishing tool, workpiece material, type of previous machining (milling, turning,…), etc. To prove this hypothesis, the authors of this paper have used an FEM analysis and experiment.

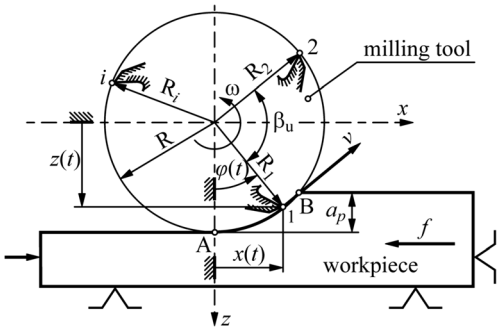

Fig. 1 Schematic diagram of the milling process

2 Theoretical model

Bearing in mind that ball burnishing is usually preceded by milling, the theoretical model of roughness was derived based on analysis of milling kinematics. A kinematic-wise milling process is performed by the main rotational movement of tool and workpiece feed. The auxiliary workpiece movement is most often linear.

If we consider a case of up milling (Fig. 1), then arc AB, which is generated by the miller tooth movement from point A to point B, at cutting speed, v, and feed rate, f, represents a segment of cycloid trajectory.

The change of angle $\varphi(t)$ is defined by the following expression:

$$\varphi(t) = \omega \cdot t \tag{1}$$

where ω is the angular cutter speed and t is the time.

Milling tooth trajectory, according to Fig. 1, can be determined based on the coordinates of the tooth cutting wedge tip, $x(t)$ and $z(t)$ [29]:

$$x(t) = R_i \cdot \sin\varphi(t) + f \cdot t \tag{2}$$

$$z(t) = R_i \cdot \cos\varphi(t) \tag{3}$$

where R_i is the radius of the ith milling tool teeth.

After substitution of $\varphi(t)$ in coordinate equations of the tooth cutting wedge tip (Eqs. 2 and 3), there follows:

$$x(t) = R_i \cdot \sin\omega \cdot t + f \cdot t \tag{4}$$

$$z(t) = R_i \cdot \cos\omega \cdot t \tag{5}$$

In real manufacturing conditions, milling is characterized by a certain radial deflection of particular cutter teeth, which are the result of cutter manufacturing and sharpening errors, and deviation between kinematic and geometric cutter axes. In such cutting conditions, the location of cutter teeth is defined by their particular radius vectors, R_i, and angle β_u (Fig. 1).

Location coordinates $x(t)$ and $z(t)$ of the ith cutter tooth are defined by equations:

$$x_i(t) = R_i \cdot \sin[\omega \cdot t + (i-1) \cdot \beta_u] + f \cdot t \tag{6}$$

$$z_i(t) = R_i \cdot \cos[\omega \cdot t + (i-1) \cdot \beta_u] \tag{7}$$

where

$$\beta_u = 2\pi / N \tag{8}$$

and N is the number of teeth on the cutting tool.

Analysis of these equations leads to the conclusion that the tooth with the greatest radius vector forms the profile of the machined surface. The diagrams of teeth travel during down milling and up milling—with the following parameters: N=3; the diameter of the milling tool d=10 mm, i.e. R_1=5.06 mm, R_2=5.04 mm and R_3=5.02 mm; v=9.4 m/min; and f=300 mm/min—are shown in Fig. 2.

The profile of the surface machined with the following parameters: d=10 mm, v=7.1 m/min and f=300 mm/min which is formed by the tooth with the greatest radius vector is shown in Fig. 3.

The theoretical model presented in Fig. 3 was used to model the surface roughness profile in the FEM simulation.

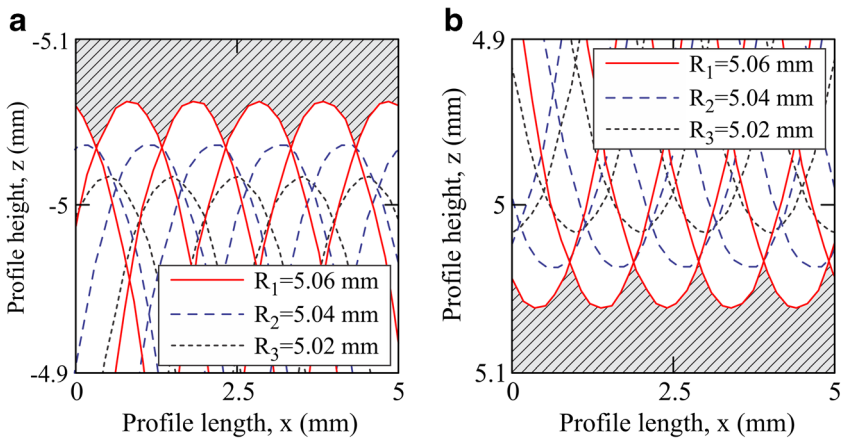

Fig. 2 Diagrams of teeth travel and surface profile, machining parameters: N=3, d=10 mm, v=9.4 m/min and f=300 mm/min, for **a** down milling and **b** up milling

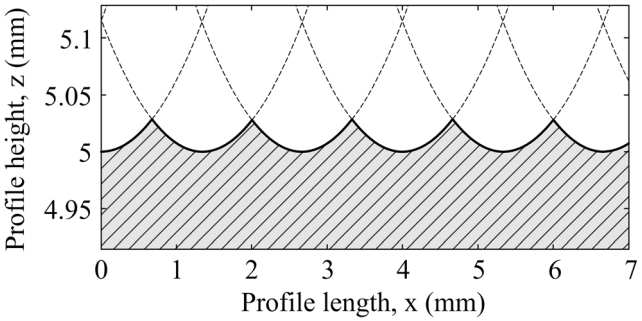

Fig. 3 Surface topography which is formed by the tooth with the greatest radius vector, machining parameters: d=10 mm, v=7.1 m/min and f=300 mm/min

Table 1 Numerically obtained surface roughness parameters before and after burnishing

Position	δ (μm)	Ra (μm)	Rp (μm)	Rv (μm)	Rz (μm)
Initial roughness	–	10.90	22.76	12.34	35.10
1	5	8.94	20.25	11.38	31.63
2	10	8.73	18.87	11.35	30.22
3	15	8.06	13.38	10.88	24.26
4	20	6.63	11.41	10.07	21.48
5	25	4.04	6.31	7.85	14.16
6	30	4.26	6.01	17.69	23.70
7	35	6.82	20.27	18.92	39.19

3 Simulation of ball burnishing process

Software, Simufact Forming 11.0, was used to model the ball burnishing process. A 2-D FEM analysis was performed by varying the depth of burnishing ball penetration into the workpiece material. The considered theoretical surface roughness profile has an initial maximum profile height of Rz=35.10 μm, where maximum valley depth is Rv=12.34 μm, maximum peak height Rp=22.76 μm and arithmetic mean surface roughness Ra=10.90 μm. The workpiece material is aluminium alloy EC1350.

The model used to simulate the process of ball burnishing consists of three components (Fig. 4a): the workpiece, support on which the workpiece is rested, i.e. machine worktable, and the burnishing ball, which rolls across the workpiece surface. The burnishing ball diameter was 6 mm. The ball model was additionally refined using Surface Remesh, in order to eliminate initial surface imperfections, which are the result of imperfect triangulation done by the CAD software during file export. The resulting ball mesh is very smooth as can be seen in Fig. 4b. The ball was considered a rigid body.

The workpiece model was meshed using a Quadtree mesher with a Quad (10) type of FE. The mesh consists of 107,641 FEs. It should be noted that the area of special interest—up to 0.7-mm penetration depth—was refined to allow FEs to have an edge length of 7 μm (Fig. 4c and zoom view in Fig. 4d). The surface roughness profile consists of several consecutive roughness peaks, which all have identical dimensions, as shown in Fig. 4. The transition mesh zone (Fig. 4c), approximately 0.5 mm, is situated between the refined mesh zone and the rest of the coarser mesh. The workpiece and the support are restrained in all three axes. During simulation, the friction coefficient μ between the ball and the burnished surface is set to zero (μ=0).

Simulation was performed in two stages. The process of burnishing ball penetration into the workpiece material up to the desired depth (marked as path I in Fig. 4a) was performed

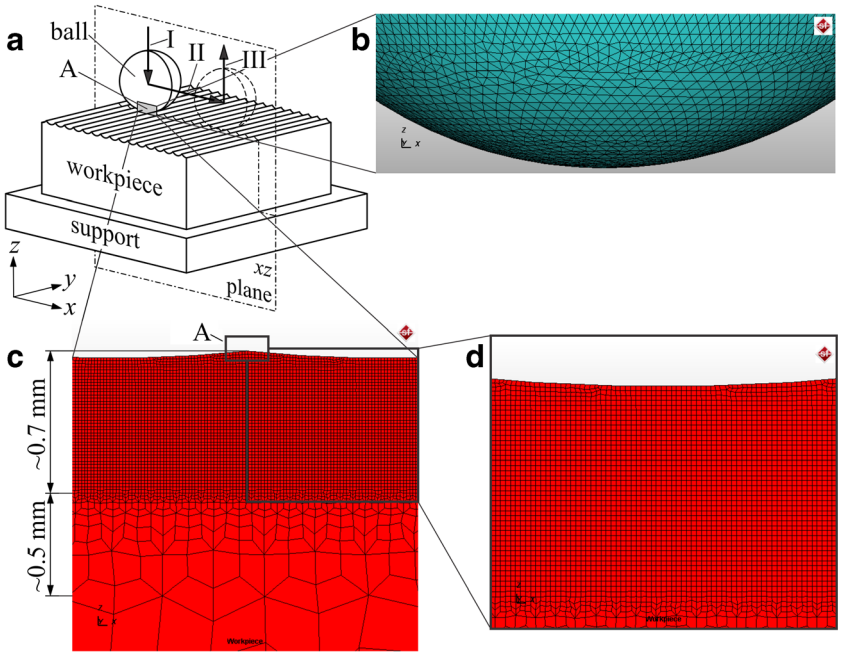

Fig. 4 Model used for FEM analysis: **a** CAD model, **b** ball mesh, **c** workpiece mesh in *xz* plane and **d** zoom view of workpiece mesh

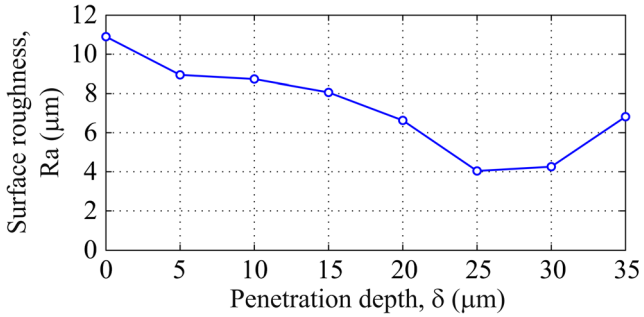

Fig. 5 Relationship between surface roughness, Ra, and the ball penetration depth, δ, into workpiece material

during the first stage, at contact point A, as shown in Fig. 4a, c. It is important to note that the initial contact between the ball and workpiece is established at the profile point with the greatest z-coordinate; i.e. the initial contact is established at the peak of the theoretical roughness profile. The second part of this simulation covered the very process of ball burnishing, where the ball rolls across the workpiece surface at a predefined speed (marked as path II in Fig. 4a). The ball covers the distance equal to five consecutive surface roughness peaks. The load, received by the roughness asperity during the first stage of the simulation, is, by its nature, different from that received by other roughness asperities during the second stage of simulation. For this reason, the results pertaining to surface topography and stress distribution of the first surface asperity are disregarded. After burnishing, the ball is lifted up (marked as path III in Fig. 4a).

4 Results

Seven numerical simulations were performed. The ball depth penetration into the workpiece material, δ, was varied within the 5–35-μm range, with 5-μm increments, in order to cover the maximum surface roughness height, Rz=35 μm. In Table 1, the numerically obtained values of surface roughness parameters Ra, Rp, Rv and Rz as the function of the depth of ball penetration are shown. Based on the results of FEM simulations, a relationship between ball penetration depth, δ, and the change of surface roughness, Ra, was established (Fig. 5).

The best result from the aspect of Ra improvement was achieved for δ=25 μm, when the initial surface roughness of Ra=10.9 μm was reduced to Ra=7.4 μm. Moreover, the improvements were also observed when the penetration depth was smaller than the maximum surface roughness profile peak height, Rp. For small penetration depths (δ=5 μm and δ=10 μm) as well as for penetration depths exceeding Rp (δ=35 μm), the improvements of surface roughness were lower.

Comparisons of surface roughness profiles obtained by the model used in simulations and the resulting roughness profiles obtained by simulations performed with various ball penetration depths are shown in Fig. 6. Figure 6 clearly shows the way that the roughness peaks are deformed under ball pressure. The peaks get lower while the profile widens and fills the space in-between, where the material flows immediately before the burnishing ball, in the direction of the feed.

Figure 7 shows the material ratio curves for ball burnishing up to a ball penetration depth of 25 μm. According to the presented results, it could be concluded that the burnishing process improves the material ratio curve.

Analysis of numerical simulations, in terms of internal residual stresses within the workpiece after ball burnishing, shows that stress distribution over workpiece depth also depends on the depth of ball penetration into the workpiece. Von Mises stresses have been considered. Shown in Fig. 8 are the distributions of residual stresses in the workpiece surface layer after ball burnishing. Maximum stresses occur immediately below the workpiece surface. Residual stresses are registered up to depths of 0.1, 0.2, 0.5 and 1 mm from the surface. The increase of ball penetration depth increases the residual stresses in the workpiece surface layer, as illustrated in Fig. 9. Considering the magnitudes of maximal residual stresses, they range from 70 MPa for δ=5 μm to 130 MPa for δ=35 μm.

In order to verify the results obtained by FEM analysis, experimental investigations of ball burnishing using an especially designed high-stiffness burnishing tool [9] were conducted on a CNC milling machine (Fig. 10a). The tool design features three roller bearings and allows the burnishing ball to be supported at three points and freely roll on the plane. An experimental investigation of the burnishing process was

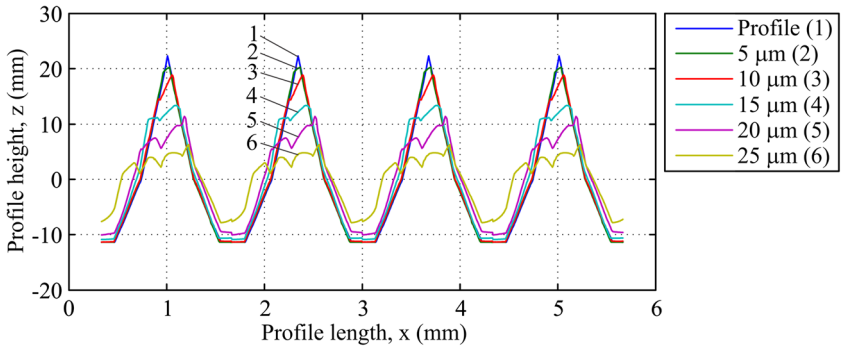

Fig. 6 Superposition of the initial surface roughness profile and the resulting roughness profiles after ball burnishing at various depths of ball penetration

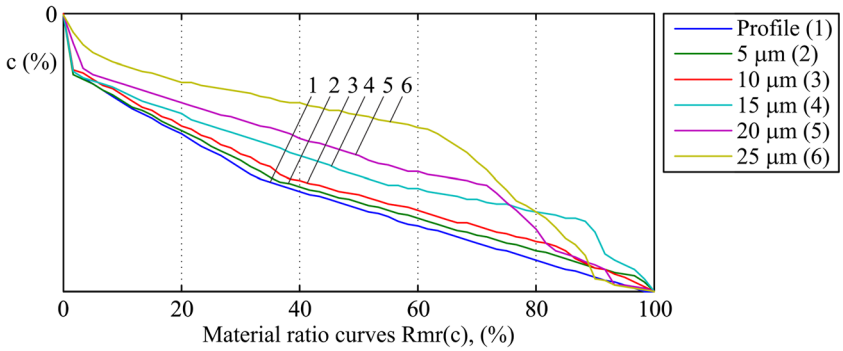

Fig. 7 Material ratio curves for different ball penetration depths

conducted on a flat plate with dimensions 62×62×25 mm. The plate was made of aluminium EN AW-6082 (AlMgSi1) T651, having 89 HB hardness. The chemical composition of the material was as follows: 0.9 % Si, 0.5 % Fe, 0.1 % Si, 0.6 % Mn, 0.9 % Mg, 0.25 % Cr, 0.2 % Zn, 0.1 % Ti, other elements 0.15 % and the remaining content of Al. The mechanical parameters for this material correspond to the parameters of the material used in the numerical simulations. In this experiment, a 7-mm-diameter burnishing ball was made of steel A 295 52100 (USA/ASTM). The ball hardness and surface roughness were 65 HRC and Ra=0.02 μm, respectively.

The initial surface was obtained by machining the surface with a ϕ20 end-milling cutter. The ball burnishing was performed in 16 fields with dimensions of 10×10 mm. The burnishing feed in all fields was f_b=0.2 mm, and burnishing tool speed was v_b=2000 mm/min. The initial depth of penetration, δ, i.e. the tool offset in the direction of z-axis, was determined before the ball burnishing procedure. The depth of penetration in the first field was approximately 2 μm. In each following field, the penetration depth was increased by 2 μm, so the penetration depth in the last tested field was δ=32 μm. The other test conditions were the same for all tested fields. A photograph of the plate after the experiment is shown in Fig. 10b.

The surface roughness parameters, before and after burnishing, were measured using a Rank Taylor Hobson Talysurf 6 profiler. The selected evaluation profile length was 4 mm. The values of surface roughness parameters Ra, Rp, Rv and Rz, depending on the depth of penetration of the ball, δ, are given in Table 2.

Diagram of the variation of surface roughness, Ra, as a function of penetration depth, δ, is presented in Fig. 11.

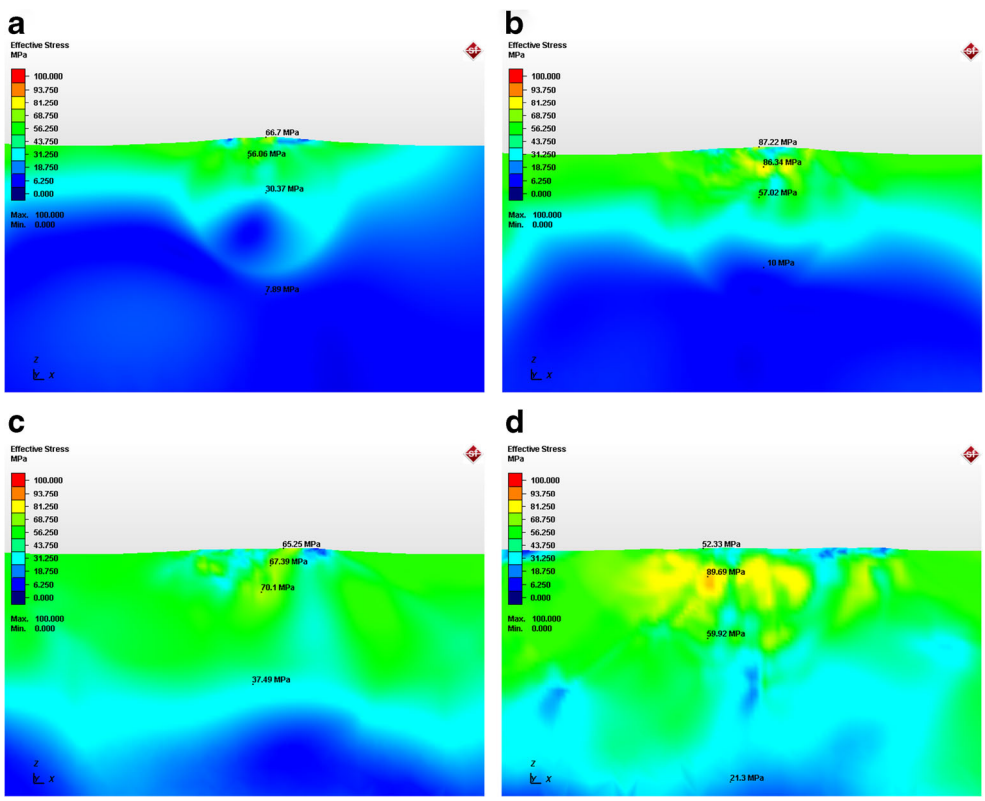

Fig. 8 Residual stresses within workpiece after ball burnishing at various ball penetration depths: **a** δ=10 μm, **b** δ=15 μm, **c** δ=20 μm and **d** δ=30 μm

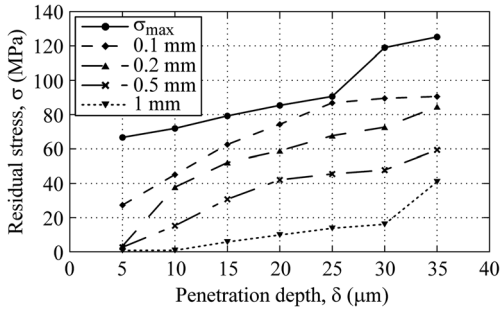

Fig. 9 Dependence of residual stresses in the workpiece surface layer on the ball penetration depth at various depths from surface layer

Analysis of the diagram in Fig. 11 shows that higher penetration depth, δ, leads to a reduction of Ra, up to a certain limit, after which Ra continues to grow as the penetration depth increases. Minimum Ra is obtained for penetration depth δ=16 μm which is near to the maximum profile peak height of initial surface roughness Rp=15.4 μm. The results obtained are in strong agreement with the results of the FEM analysis shown in Fig. 5.

Figure 12a shows the overlap of the initial surface profile and the surface profile after ball burnishing with a penetration depth of δ=16 μm.

Shown in Fig. 12b are the superimposed surface roughness profiles and the burnishing ball in real scale. The angular speed of the ball is ω_b while the burnishing feed is f_b. The ball is shown in the position where the penetration depth equals the surface roughness peak height, Rp. It is assumed that under ball burnishing, a plastic flow of material from the peaks to the valleys in the surface occurs. Because of plastic flow, material from the peak (marked as area Ap in Fig. 12b) will fill in the next valley (marked as area Av in Fig. 12b), thus reducing the overall surface roughness.

5 Discussion

Assumptions claiming that near-maximal surface quality, in terms of Ra, can be achieved when the tool penetrates material to the depth which approximately equals the maximum peak height, Rp, have been confirmed by numerical simulations and experimental investigations. Based on the numerical verification of results, the authors maintain that penetrations into roughness peaks, which exceed Rp, do not significantly contribute to the increase of surface quality. The primary reason is that, in this case, the displaced material would probably create additional roughness peaks. Results obtained by FEM analysis also show that, during deformations, i.e. the plastic flow of surface roughness profile peaks, the roughness profile becomes lower. The empty space between peaks gets filled up, where a part of the material flows immediately in front of the burnishing ball, in the direction of the feed. It has been established that the lowest Ra is obtained when the ball is impressed into the workpiece material up to the depth that approximately corresponds to the maximum peak height, Rp. This can be especially important when burnishing surfaces were previously relatively rough.

Due to complexity of the ball burnishing simulation process [21] and in order to avoid possible error due to adoption of the virtually unknown ball/workpiece friction coefficient, the friction coefficient between the ball and the burnished

Table 2 Experimentally obtained surface roughness parameters before and after burnishing

Position	δ (μm)	Ra (μm)	Rp (μm)	Rv (μm)	Rz (μm)
Initial roughness	–	2.91	15.4	14.8	31.2
1	2	1.78	7.4	8.9	16.3
2	4	1.22	4.7	5.3	10.0
3	6	1.08	2.8	5.7	8.5
4	8	0.74	2.0	2.3	4.3
5	10	0.49	1.1	5.7	6.8
6	12	0.53	2.8	3.7	6.5
7	14	0.50	1.4	1.8	3.2
8	16	0.33	1.2	1.2	2.4
9	18	0.61	4.2	2.3	6.5
10	20	0.64	3.8	5.8	9.6
11	22	0.58	3.0	1.5	4.5
12	24	0.71	5.5	2.0	7.5
13	26	1.09	2.5	4.3	6.8
14	28	0.98	1.7	4.6	6.3
15	30	0.85	2.0	5.1	7.1
16	32	0.86	2.0	4.1	6.1

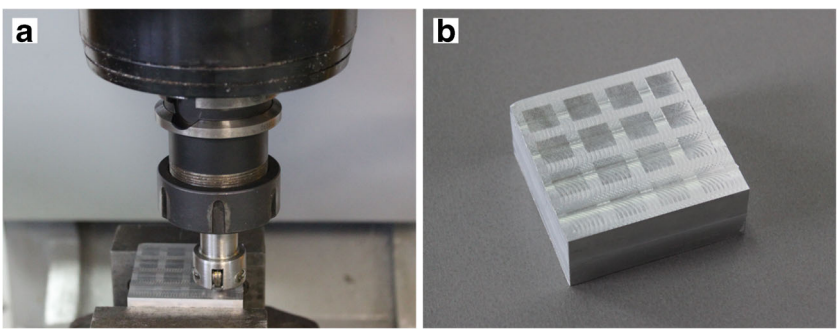

Fig. 10 Photographs made during experimental investigations: **a** plate mounted on CNC milling machine and **b** plate after ball burnishing

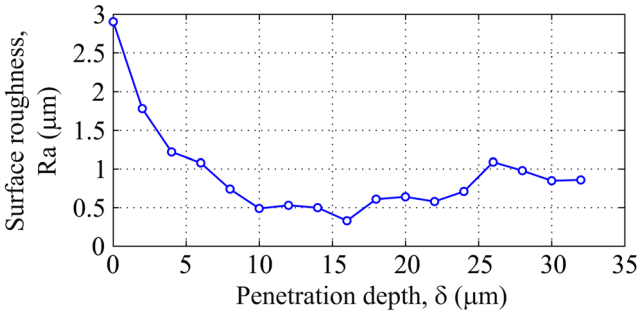

Fig. 11 Dependence of surface roughness, Ra, on various ball penetration depths, δ, during experimental investigation

surface was set to zero (μ=0). However, in the real process, this coefficient is larger than zero (μ>0). Regardless of the adopted value (μ=0), the numerical simulations yielded valid results which are in compliance with experimental results (Figs. 5 and 11).

Based on the stress analysis, it is possible to see that by burnishing at depths of penetration that reach maximum peak height, high internal compressive stresses, reaching up to 130 MPa, develop in the workpiece surface layer. Bearing in mind that the material used in numerical simulations was aluminium alloy whose yield stress is about 60 MPa, it is possible to conclude that high compressive stresses in the workpiece surface layer can be attributed to the phenomenon of peeling. The peeling of surface layers after ball burnishing has so far been associated with bad tool design solutions, which failed to provide free ball rolling across the workpiece surface, which resulted in slipping. Surface peeling has also been observed when ball burnishing was performed with elastic tools, due to oversized burnishing force or due to the excessive number of passes with the burnishing tool. It is too early to claim that high internal compressive stresses due to excessive ball penetration depth (greater than maximum peak height, Rp) cause peeling in workpiece surface layers. However, this could be further investigated in future work.

6 Conclusion

Based on theoretical considerations and the performed FEM simulations and experimental investigations, it is possible to draw several conclusions:

- The presented theoretical model of the previously machined workpiece surface profile is kinematically compatible with that obtained for the side and face milling cutter.
- The model of the previously machined workpiece was used to simulate the ball burnishing process in Simufact Forming software. The simulations were performed with various ball penetration depths.
- Based on the simulation results, it has been established that minimal surface roughness, Ra, is obtained for ball penetration depth which is close to the maximum peak height, Rp.
- Von Mises stress field distribution in the workpiece surface layer was also obtained. As the ball penetration depth increases, so do the internal stress values.
- Experimental investigations of the ball burnishing process were performed using a workpiece with a previously milled surface. Theoretically, the real face and side miller

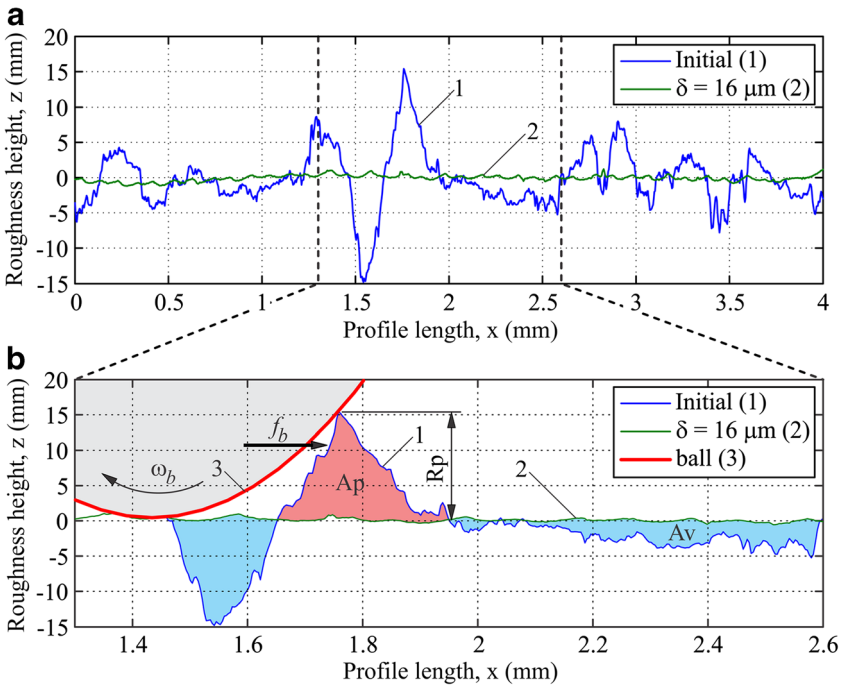

Fig. 12 Roughness profiles: **a** before and after ball burnishing and **b** zoom view with detail of plastic flow of surface roughness peak

yields surface roughness which is different to that obtained by the simulation of the ball burnishing process.

- Regardless of the fact that the experimental investigation and FEM simulation used two different cutting tools with different workpiece surface penetrations, as well as the fact that the initial workpiece surface roughness differed, identical results were obtained.
- Both, the experimental and simulation results indicate that the minimal surface roughness (expressed by Ra) was achieved by using a ball burnishing penetration depth close to the maximum peak height, Rp. This fact strongly implies that the minimum surface roughness, Ra, is obtained for penetration depths close to Rp, regardless of the tool used for initial machining and the initial workpiece surface roughness.
- It is highly possible that ball penetration depths close to Rp create the most favourable conditions for material flow, from profile peak heights towards the valleys. The valleys with the depth of Rp allow sufficient free volume to be filled up by material flowing from the peaks. Moreover, there is no excessive material expulsion and, therefore, no increase in surface roughness.

Future investigations shall be directed towards determination of optimal ball penetration depth for various workpiece materials. Efforts shall also be made to draw more general conclusions based on the experimental results.

References

1. Bouzid W, Tsoumarev O, Sai K (2004) An investigation of surface roughness of burnished AISI 1042 steel. Int J Adv Manuf Technol 24:120–125
2. Bougharriou A, Bouzid Sai W, Sai K (2010) Prediction of surface characteristics obtained by burnishing. Int J Adv Manuf Technol 51:205–215
3. Li FL, Xia W, Zhou ZY, Zhao J, Tang ZQ (2012) Analytical prediction and experimental verification of surface roughness during the burnishing process. Int J Mach Tool Manuf 62:67–75
4. Gharbi F, Sghaier S, Hamdi H, Benameur T (2012) Ductility improvement of aluminum 1050A rolled sheet by a newly designed ball burnishing tool device. Int J Adv Manuf Technol 60:87–99
5. Bougharriou A, Bouzid W, Sai K (2014) Analytical modeling of surface profile in turning and burnishing. Int J Adv Manuf Technol 75:547–558
6. Rao DS, Hebbar HS, Komaraiah M (2007) Surface hardening of high-strength low alloy steels (HSLA) dual-phase steels by ball burnishing using factorial design. Mater Manuf Process 22:825–829
7. Abu Shreehah TA (2008) Developing and investigating of elastic ball burnishing tool. Int J Adv Manuf Technol 36:270–279
8. Sagbas A (2011) Analysis and optimization of surface roughness in the ball burnishing process using response surface methodology and desirability function. Adv Eng Softw 42:992–998
9. Tadic B, Todorovic MP, Luzanin O, Miljanic D, Jeremic MB, Bogdanovic B, Vukelic D (2013) Using specially designed high-stiffness burnishing tool to achieve high-quality surface finish. Int J Adv Manuf Technol 67:601–611
10. El-Taweel TA, El-Axir MH (2009) Analysis and optimization of the ball burnishing process through the Taguchi technique. Int J Adv Manuf Technol 41:301–310
11. Esme U (2010) Use of grey based Taguchi method in ball burnishing process for the optimization of surface roughness and microhardness of AA 7075 aluminum alloy. Mater Tehnol 44:129–135
12. Babu PR, Ankamma K, Prasad TS, Raj AVS, Prasad NE (2012) Optimization of burnishing parameters and determination of select surface characteristics in engineering materials. Sadhana-Acad Proc Eng Sci 37:503–520
13. Revankar GD, Shetty R, Rao SS, Gaitonde VN (2014) Analysis of surface roughness and hardness in ball burnishing of titanium alloy. Measurement 58:256–268
14. Esme U, Sagbas A, Kahraman F, Kulekci MK (2008) Use of artificial neural networks in ball burnishing process for the prediction of surface roughness of AA 7075 aluminum alloy. Mater Tehnol 42:215–219
15. Ibrahim AA, Abd Rabbo SM, El-Axir MH, Ebied AA (2009) Center rest balls burnishing parameters adaptation of steel components using fuzzy logic. J Mater Process Technol 209:2428–2435
16. Basak H, Goktas HH (2009) Burnishing process on al-alloy and optimization of surface roughness and surface hardness by fuzzy logic. Mater Des 30:1275–1281
17. Esme U, Kulekci MK, Ozgun S, Kazancoglu Y (2013) Predictive modelling of ball burnishing process using regression analysis and neural network. Mater Test 55:187–192
18. Stalin John MR, Vinayagam BK (2014) Optimization of nonlinear characteristics of ball burnishing process using Sugeno fuzzy neural system. J Braz Soc Mech Sci Eng 36:101–109
19. Sarhan AAD, El-Tayeb NSM (2014) Investigating the surface quality of the burnished brass C3605—fuzzy rule-based approach. Int J Adv Manuf Technol 71:1143–1150
20. Bouzid Sai W, Sai K (2005) Finite element modeling of burnishing of AISI 1042 steel. Int J Adv Manuf Technol 25:460–465
21. Balland P, Tabourot L, Degre F, Moreau V (2013) Mechanics of the burnishing process. Precis Eng 37:129–134
22. Sayahi M, Sghaier S, Belhadjsalah H (2013) Finite element analysis of ball burnishing process: comparisons between numerical results and experiments. Int J Adv Manuf Technol 67:1665–1673
23. Grochała D, Berczynski S, Grzadziel Z (2014) Stress in the surface layer of objects burnished after milling. Int J Adv Manuf Technol 72:1655–1663
24. Mohammadi F, Sedaghati R, Bonakdar A (2014) Finite element analysis and design optimization of low plasticity burnishing process. Int J Adv Manuf Technol 70:1337–1354
25. El-Axir MH (2007) An investigation into the ball burnishing of aluminium alloy 6061-T6. Proc Inst Mech Eng B J Eng Manuf 221:1733–42
26. El-Tayeb NSM, Low KO, Brevern PV (2008) Enhancement of surface quality and tribological properties using ball burnishing process. Mach Sci Technol 12:234–48
27. Grzesik W, Zak K (2013) Producing high quality hardened parts using sequential hard turning and ball burnishing operations. Precis Eng 37:849–855
28. Vukelic D, Miljanic D, Randjelovic S, Budak I, Dzunic D, Eric M, Pantic M (2013) A burnishing process based on the optimal depth of workpiece penetration. Mater Tehnol 47:43–51
29. Tadic B (1997) Model research of up milling process from the aspects of dynamics and tribology. Dissertation, University of Kragujevac